



(12) EUROPEAN PATENT APPLICATION

(43) Date of publication:
03.03.1999 Bulletin 1999/09

(51) Int Cl.⁶: H04L 1/20

(21) Application number: 98306614.3

(22) Date of filing: 18.08.1998

(84) Designated Contracting States:
AT BE CH CY DE DK ES FI FR GB GR IE IT LI LU
MC NL PT SE
Designated Extension States:
AL LT LV MK RO SI

• Kadaba, Srinivas R.
Chatham, New Jersey 07928 (US)
• Nanda, Sanjiv
Plainsboro, New Jersey 08536 (US)
• Ejzak, Richard Paul
Wheaton, Illinois 60187 (US)

(30) Priority: 25.08.1997 US 921454

(71) Applicant: LUCENT TECHNOLOGIES INC.
Murray Hill, New Jersey 07974-0636 (US)

(74) Representative:
Buckley, Christopher Simon Thirsk et al
Lucent Technologies (UK) Ltd,
5 Mornington Road
Woodford Green, Essex IG8 0TU (GB)

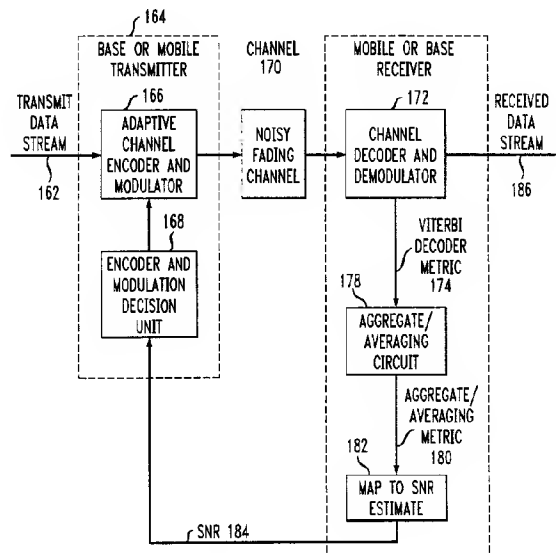
(72) Inventors:
• Balachandran, Krishna
Middletown, New Jersey 07748 (US)

(54) System and method for measuring channel quality information

(57) In a system and method to measure channel quality in terms of signal to noise ratio for the transmission of coded signals over fading channels, a Viterbi decoder metric for the Maximum Likelihood path is used as a channel quality measure. This Euclidean distance metric is filtered in order to smooth out short term variations. The filtered or averaged metric is a reliable chan-

nel quality measure which remains consistent across different coded modulation schemes and at different mobile speeds. The filtered metric is mapped to the signal to noise ratio per symbol using a threshold based scheme. Use of this implicit signal to noise ratio estimate is used for the mobile assisted handoff and data rate adaptation in the transmitter.

FIG. 11



Description**BACKGROUND OF THE INVENTION**5 **1. FIELD OF THE INVENTION**

[0001] The present invention relates generally to the field of communication systems and, more particularly, to communications systems which measure the quality of channel information.

10 **2. DESCRIPTION OF THE RELATED ART**

[0002] As the use of wireless communications continues to grow worldwide at a rapid pace, the need for frequency spectrum efficient systems that accommodate both the expanding number of individual users and the new digital features and services such as facsimile, data transmission, and various call handling features has increased.

15 [0003] Current wireless data systems such as the cellular digital packet data (CDPD) system and the IS-130 circuit switched time division multiple access data system support only low fixed data rates which are insufficient for several applications. Because cellular systems are engineered to provide coverage at the cell boundary, the signal to interference plus noise ratio (SNR) over a large portion of a cell is sufficient to support higher data rates. Adaptive data rate schemes using bandwidth efficient coded modulation are currently have been proposed for increasing data throughput
20 over the fading channels encountered in cellular systems. Increased data throughput is accomplished by using bandwidth efficient coded modulation schemes with higher information rates. However, a practical problem to using these schemes is to dynamically adjust the coded modulation to adapt to the channel conditions.

[0004] At present, there is a need to determine the channel quality based on the measurements or metrics of the SNR or the achievable frame error rate (FER) for the time varying channel. However, in cellular systems there is no
25 fast accurate method to measure either the SNR or to estimate the FER.

[0005] The difficulty in obtaining these metrics in a cellular system is due to the time varying signal strength levels found on the cellular channel. The time varying signal strength levels, sometimes referred to as fading, are the result of the movement of the mobile station or cellular phone relative to the base station (also known as a cell site). Recent schemes propose a short term prediction of the FER, but not the SNR, using the metric for the second best path by a
30 Viterbi decoder. This metric is computationally very intensive and reacts to short term variations in fading conditions. Therefore, there is a need, in the field of wireless communication systems, for a method accurately measuring the channel quality in terms of the SNR.

[0006] It is also important to measure channel quality, in terms of SNR or FER, for the purpose of mobile assisted handoff (MAHO). However, FER measurements are usually very slow for the purpose of handoff or rate adaptation.
35 FER as a channel quality metric is slow because it can take a very long time for the mobile to count a sufficient number of frame errors. Therefore, there is a need for a robust short term channel quality indicator that can be related to the FER.

[0007] As a result, channel quality metrics such as symbol error rate, average bit error rate and received signal strength measurements have been proposed as alternatives. The IS-136 standard already specifies measurement procedures for both bit error rate and received signal strength. However, these measures do not correlate well with
40 the FER, or the SNR, which is widely accepted as the meaningful performance measure in wireless systems. Also, received signal strength measurements are often inaccurate and unreliable. The present invention is directed to overcoming, or at least reducing the effects of one or more of the problems set forth above.

SUMMARY OF THE INVENTION

45 [0008] In accordance with one aspect of the present invention there is provided a system and method for determining the signal to noise ratio which provides for establishing a set of path metrics corresponding to a set of predetermined signal to noise ratios. A digital signal is received and a path metric determined for the digital signal. Mapping of the path metric is provided to a corresponding signal to noise ratio in the set of predetermined signal to noise ratios.

50 [0009] These and other features and advantages of the present invention will become apparent from the following detailed description, the accompanying drawings and the appended claims.

BRIEF DESCRIPTION OF THE DRAWINGS

55 [0010] The advantages of this invention will become apparent upon reading the following detailed description and upon reference to the drawings in which:

FIG. 1 is a graphical representation of three cell sites within a cluster;

FIG. 2 is a block diagram of both the base station and the mobile station transmitters and receivers for the present invention;

FIG. 3 is a block diagram of a decoder system for present invention;

FIG. 4 is a graph having a curve, with the vertical scale representing the average Viterbi decoder metric and the horizontal scale representing the time slot pair (block) number;

FIG. 5 is a graph having a curve, with the vertical scale representing the average Viterbi decoder metric and the horizontal scale representing the SNR;

FIG. 6 is a flow diagram illustrating the steps performed during the process of determining the SNR using the lookup table and adjusting the coded modulation scheme used by the system;

FIG. 7 is a flow diagram illustrating the steps performed during the process of determining the SNR using the linear prediction and adjusting the coded modulation scheme used by the system;

FIG. 8 is a graph having a three curves, with the vertical scale representing the \overline{FER} and the horizontal scale representing the SNR;

FIG. 9 is a table of values for a conservative mode adaptation strategy based on a Viterbi algorithm metric average;

FIG. 10 is a table of values for an aggressive mode adaptation strategy based on a Viterbi algorithm metric average;

FIG. 11 is a block diagram of both the base station and the mobile station transmitters and receivers for the implementation of an adaptive coding scheme; and

FIG. 12 is a block diagram of both the base station and the mobile station transmitters and receivers for the implementation of a mobile handoff scheme.

DETAILED DESCRIPTION

[0011] Referring to the drawings and initially to FIG. 1, a plurality of cells 2, 4, and 6 in a telecommunications system are shown. Consistent with convention, each cell 2, 4, and 6 is shown having a hexagonal cell boundary. Within each cell 2, 4, and 6 are base stations 8, 10, and 12 that are located near the center of the corresponding cell 2, 4, and 6. Specifically, the base station 8 is located within cell 2, base station 10 is located within cell 4, and base station 12 is located within cell 6.

[0012] The boundaries 14, 16 and 18 separating the cells 2, 4, and 6 generally represent the points where mobile assisted handoff occurs. As an example, when a mobile station 20 moves away from base station 8 towards an adjacent base station 10, the SNR from the base station 8 will drop below a certain threshold level past the boundary 14 while, at the same time, the SNR from the second base station 10 increases above this threshold as the mobile station 20 crosses the boundary 14 into cell 4. Cellular systems are engineered to provide coverage from each base station up until the cell boundary. Thus, the SNR over a large portion of a cell 2 is sufficient to support higher data rates because the SNR from the base station 8 is greater than the minimum SNR needed to support the data transfer at the boundary 14. FIG. 2 is an example implementation of an adaptive rate system which takes advantage of this support for higher data rates.

[0013] FIG. 2 is a block diagram for the schematic of the base station 8 and the mobile station 20 for the invention. The base station 8 consists of both an adaptive rate base station transmitter 22 and an adaptive rate base station receiver 24. Likewise, the mobile station 20 also consists of both an adaptive rate mobile station receiver 26 and an adaptive rate mobile transmitter 28. Each pair of the transmitter and the receiver, corresponding to either the base station 8 or mobile station 20, are in radio connection via a corresponding channel. Thus, the adaptive rate base station transmitter 22 is connected through a downlink radio channel 30 to the adaptive rate mobile receiver 26 and the adaptive rate mobile station transmitter 28 is connected through an uplink radio channel 32 to the adaptive rate base station receiver 24. This implementation allows for increased throughput between the base station 8 and the mobile station 20 over both the downlink channel 30 and the uplink channel 32 because of the use of adaptive bandwidth efficient coded modulation schemes.

[0014] Thus, the information rate may be varied by transmitting at a fixed symbol rate (as in IS-130/IS-136), and changing the bandwidth efficiency (number of information bits per symbol) using a choice of coded modulation schemes.

However, coded modulation schemes with different bandwidth efficiencies have different error rate performance for the same SNR per symbol. At each SNR, the coded modulation scheme is chosen which results in the highest throughput with acceptable FER and retransmission delay. Therefore, detection of channel quality in terms of SNR or achievable FER is very important for this invention. Both the SNR and FER as channel quality metrics can be derived from the cumulative Euclidean distance metric corresponding to a decoded received sequence.

[0015] A block diagram of an encoder and decoder system for the invention is shown in FIG. 3. Within the transmitter 34, the information sequence $\{a_k\}$ 36 is encoded using a convolutional encoder 38 to provide a coded sequence $\{b_k\}$ 40. The coded sequence $\{b_k\}$ 40 is then mapped through a symbol mapper 42 to a symbol $\{s_k\}$ 44 from either an M-ary constellation such as M-ary phase shift keying (PSK) or a M-ary quadrature amplitude modulation (QAM) scheme using either a straightforward Gray mapping or a set partitioning technique. Puleshaping is then carried out using transmit filters 46 that satisfy the Gibby Smith constraints (i.e. necessary and sufficient conditions for zero intersymbol interference). The symbol $\{s_k\}$ 44 is then transmitted through the channel 48 to the receiver 50. At the receiver 50, the front end analog receive filters 52 are assumed to be matched to the transmit filters 46 and the output $\{r_k\}$ 54 is sampled at the optimum sampling instants.

[0016] The received symbol at the k^{th} instant is given by

$$r_k = \alpha_k s_k + n_k,$$

where s_k denotes the complex transmitted symbol $\{s_k\}$ 44, α_k represents the complex fading channel 64 coefficient and n_k denotes the complex additive white Gaussian noise (AWGN) with variance N_0 . For this example, the fading channel 64 is assumed to be correlated, and may be represented by a number of models. In this example the Jakes' model for Rayleigh fading is used. The convolutional encoder 38 is chosen to optimize the systems needs. Here, a trellis code has been chosen, however, many other codes could also be used by this invention without modifying the essence of the invention. Maximum likelihood decoding at the receiver 50 may be carried out using a Viterbi algorithm circuit (also known as a maximum likelihood decoder) 56 to search for the best path through a trellis. An estimate of the complex fading channel 64 coefficients is assumed available to the decoder (i.e. the convolutional encoder 58) of the receiver 50.

[0017] The Viterbi algorithm circuit 56 associates an incremental Euclidean distance metric with each trellis branch transition and tries to find the transmitted sequence $\{s_k\}$ 44 that is closest in Euclidean distance to the received sequence $\{r_k\}$ 54. The Viterbi algorithm circuit 56 processes each possible data sequence $\{\hat{a}_k\}$ through both a convolutional encoder 58 and symbol mapper 60 to produce a possible decoded sequence decoded sequence $\{\hat{s}_k\}$ 62. The Viterbi algorithm circuit 56 then uses the received sequence $\{r_k\}$ 54 and the estimated channel coefficient $\{\hat{\alpha}_k\}$ 64 in an incremental Euclidean distance metric computation circuit 66 which computes the incremental Euclidean distance. The incremental Euclidean distance metric is then processed through a cumulative feedback loop 68 which produces the cumulative path metric 72. Next, the cumulative path metric 72 and the cumulative metrics corresponding to all possible transmitted sequences $\{\hat{a}_k\}$ 70 are input into a minimum metric processor circuit 74 which outputs both the decoded data sequence $\{\hat{a}_k\}$ 76 and the minimum metric m_i for the i^{th} block. The cumulative path metric corresponding to the decoded sequence $\{\hat{s}_k\}$ 62 is given by

$$m_i = \min_{\hat{s}_k} \sum_{k=0}^{N-1} |r_k - \alpha_k \hat{s}_k|^2$$

where α_k 64 is the estimated fading channel coefficient at the k^{th} instant, and the trellis is assumed to terminate at a known state after every N symbols.

[0018] Thus, in accordance with one aspect of the present invention, the Viterbi decoder is used to derive the channel quality information from the cumulative Euclidean distance metric corresponding to the decoded trellis path for each block. However, as noted earlier, the Euclidean distance metric has large variations from one block to another in the presence of a fading channel. Thus smoothing, such as averaging, of these variation is required to obtain a good estimate of the metric. A small cumulative Euclidean distance metric would indicate that the received sequence is very close to the decoded sequence. For well designed trellis codes, this situation would only occur under good channel conditions with high SNR. Under poor channel conditions, the metric is much higher. Thus, a good estimate of the metric can be obtained at the i^{th} block of N symbols by using the following relationship:

$$M_i = \alpha M_{i-1} + (1 - \alpha) m_i$$

for α greater than zero and less than 1.0, where m_i represents the decoded trellis path metric and α represents the filter coefficient which determines the variance of the estimate.

[0019] FIG. 4, illustrates a graph having a four curves, with the vertical scale representing the average Viterbi decoder metric M_i and the horizontal scale representing the block number. The solid line curves 80 - 86 represent the time evolution of the filtered Viterbi decoder metric for a trellis coded 8 PSK scheme and a filter coefficient α equal to 0.9. An IS-130/IS-136 time slot structure ($N = 260$ symbols) is assumed and the trellis is terminated at the end of each time slot pair. The SNR ranges from 30 dB to 16 dB and is decremented in steps of 2 dB after every 600 time slot pairs. Each solid line curve represents a different combination of f_d , the doppler frequency, multiplied by T , the symbol duration. Therefore, the solid line curve parameters are as follows: (a) $f_d T = 0.0002$ for solid line curve 80; (a) $f_d T = 0.0012$ for solid line curve 82; (a) $f_d T = 0.0034$ for solid line curve 84; and (a) $f_d T = 0.0069$ for solid line curve 86. From FIG. 4, it is clear that there exists a straightforward one to one mapping between the average Euclidean distance metric M_i and the SNR. It maintains a steady level when the SNR is fixed and increases when the SNR decreases.

[0020] FIG. 5 shows a graph having four curves, with the vertical scale representing the long term average Viterbi decoder metric μ (the expected value of M_i) and the horizontal scale representing the SNR. Again, as in FIG. 4, the four curves 88 - 94 represent different doppler frequencies. From FIG. 5, it is clear that the average metric μ does not depend on the mobile speed. As a result, the long term cumulative metric average, μ , is the target metric for the present invention. Thus, once the Euclidean metric has been obtained it can be either mapped to the corresponding SNR in a lookup table or through a linear prediction approach.

[0021] The long term cumulative metric average μ and the SNR satisfy the empirical relationship

$$SNR = 10 \log_{10} \frac{NE_s}{\mu} \text{ in dB,}$$

where E_s is the average energy per transmitted symbol and N is the number of symbols per block. This behavior remains identical across the different coded modulation schemes. Therefore, the average Viterbi decoder metric provides a very good indication of the SNR. Furthermore, the short term average of the metric may be determined using the above mentioned relationship $M_i = \alpha M_{i-1} + (1 - \alpha) m_i$ FIG. 4 shows that the short term average satisfies

$$\theta_{low} < \frac{M_i}{\mu} < \theta_{high}$$

where the target metric, μ , is obtained from

$$SNR = 10 \log_{10} \frac{NE_s}{\mu}.$$

The thresholds, θ_{low} and θ_{high} depend on the standard deviation of M_i which, in turn, is a function of the filter parameter, α . Thus, the present invention incorporates two possible ways to determine the SNR from the average metric M_i .

[0022] FIG. 6 is a flow diagram describing the steps performed by either the base station or the mobile station in determining the SNR from the average metric M_i using a lookup table. The process begins in step 88 in which the cellular network determines the SNR range of interest. This SNR range is determined by the needs of the network at any given time.

[0023] The next step 98 is to generate a table of target values μ_n in descending order of SNR for the determined range of interest. Arrangement in descending order is purely for example and not a necessary or limiting aspect of the process. The target values are determined by the following relationship

$$\mu_n = \frac{NE_s}{10^{0.1(SNR_n)}}$$

for $n = 1, 2, \dots, K$, where K determines the desired granularity. In step 100, these values of μ_n versus the corresponding value of SNR are then stored into a memory unit for later use in mapping the measured values of $\frac{M_i}{\mu_n}$ to the corresponding

SNR values in the lookup table. Once the process of creating and storing the lookup table of μ_n versus SNR_n is complete, the system is then ready to receive and transmit data information.

[0024] In step 102, the receiver receives, for this example, a trellis coded signal and then decodes the received coded signal and outputs the trellis path metric m_i in step 104. For this example, the system uses a Viterbi Minimum Likelihood decoder to determine the trellis path metric m_i . Once the trellis path metric m_i is determined the system then determines M_i , the average metric for the i^{th} block, in step 106 using the relationship $M_i = \alpha M_{i-1} + (1 - \alpha) m_i$.

[0025] The process continues to decision step 108 in which a threshold detector circuit determines whether the value $\frac{M_i}{\mu_n}$ is less than the predetermined threshold θ_{low} . If the outcome of the decision step 108 is a "YES" determination, the process continues to step 110. In step 110, the system recognizes that the measured SNR is greater than the SNR_1 (the maximum SNR for the range of the lookup table). As a result, the system in step 110 clips the measured SNR to be equal to SNR_1 . Next, the system in step 112 provides the SNR value SNR_1 to the transmitter.

[0026] If the outcome of the determination step 108 is a "NO" determination, the process continues instead to decision step 114 in which a second threshold detector circuit determines whether the value $\frac{M_i}{\mu_n}$ is greater than the predetermined threshold θ_{high} . If the outcome of the decision step 114 is a "YES" determination, the process continues to step 116. In step 116, the system recognizes that the measured SNR is less than the SNR_k (the minimum SNR for the range of the lookup table). As a result, the system in step 116 clips the measured SNR to be equal to the SNR_k . Next, the system in step 112 provides the SNR value SNR_k to the transmitter.

[0027] If, on the other hand, the outcome of the determination step 114 is a "NO" determination, the process continues instead to decision step 118 in which a threshold detector circuit determines the threshold μ_n for which the value $\frac{M_i}{\mu_n}$ is both less than the predetermined threshold θ_{high} and greater than the predetermined threshold θ_{low} . The system in step 120 sets the measured SNR equal to the corresponding SNR_n for the mapped value of $\frac{M_i}{\mu_n}$ in the lookup table. As a result, the system in step 112 provides the SNR value SNR_n to the transmitter.

[0028] FIG. 7 is a flow diagram describing the steps performed by either the base station or the mobile station in determining the SNR from the average metric M , using a linear prediction process. The process begins in step 126 in which the cellular network determines the SNR range of interest. Similar to the lookup table approach describe earlier, this SNR range is first determined by the needs of the network at any given time. However, the use of a linear prediction, instead of the direct mapping of a lookup table, approach allows the receiver to react faster to the changes of SNR within the cell.

[0029] In step 126, a table of target values μ_n , in descending order of SNR, is generated for the determined range of interest. Again, arrangement in descending order is purely for example and not a necessary or limiting aspect of the process. The target values are determined by the following relationship

$$\mu_n = \frac{NE_s}{0.1(\text{SNR}_n)} \quad (35)$$

for $n = 1, 2, \dots, K$, where K determines the desired granularity. In step 128, these values of μ_n versus the corresponding value of the SNR are then stored into a first memory unit for later use in mapping the measured values of $\frac{M_i}{\mu_n}$ to the corresponding SNR values in the lookup table. Once the process of creating and storing the lookup table of μ_n versus SNR_n is complete, the system is then ready to receive and transmit data information.

[0030] In step 130, the receiver receives a coded signal, a trellis code for the example, and then decodes the received coded signal and outputs the trellis path metric m_i in step 132. Again, for this example, the system uses a Viterbi Minimum Likelihood decoder to determine the trellis path metric m_i . Once the trellis path metric m_i is determined, the system then determines M_i , the average metric for the i^{th} block in step 134 using the relationship $M_i = \alpha M_{i-1} + (1 - \alpha) m_i$. Then in step 136, the values of an optimal p^{th} order linear predictor h_l (for $l = 0, 1, \dots, p-1$) are generate and stored in to a second memory unit for later use. Next, in step 138, the process proceeds and determines the future value of \tilde{M}_{i+p} from the previous values of \tilde{M}_{i+l} using the relation

$$\tilde{M}_{i+p} = \sum_{l=0}^{p-1} h_l M_{i+l} \quad (50)$$

[0031] The process continues to decision step 140 in which a threshold detector circuit determines whether the value

$$\frac{\tilde{M}_{i+D}}{\mu_i}$$

is less than the predetermined threshold θ_{low} . If the outcome of the decision step 140 is a "YES" determination, the process continues to step 142. The system in step 142 clips the measured SNR to be equal to SNR_i . Next, the system in step 144 provides the SNR value SNR_i to the transmitter.

[0032] If the outcome of the determination step 140 is a "NO" determination, the process continues instead to decision step 146 in which a second threshold detector circuit determines whether the value

$$\frac{\tilde{M}_{i+D}}{\mu_k}$$

is greater than the predetermined threshold θ_{high} . If the outcome of the decision step 146 is a "YES" determination, the process continues to step 148. The system in step 148 clips the measured SNR to be equal to SNR_k . Next, the system in step 144 provides the SNR value SNR_k to the transmitter.

[0033] If, on the other hand, the outcome of the determination step 146 is a "NO" determination, the process continues instead to decision step 150 in which a threshold detector circuit determines whether the value

$$\frac{\tilde{M}_{i+D}}{\mu_n}$$

is both less than the predetermined threshold θ_{high} and greater than the predetermined threshold θ_{low} . The system in step 152 sets the measured SNR equal to the corresponding SNR_n for the mapped value of

$$\frac{\tilde{M}_{i+D}}{\mu_n}$$

in the lookup table. As a result, the system in step 144 provides the SNR value SNR_n to the transmitter.

[0034] This linear prediction approach helps the receiver use the current value and $p-1$ past values of the average metric to predict the channel quality metric D blocks in the future. Thus, this allows the receiver to react quickly to changes in the SNR.

[0035] While SNR is the preferred performance measure in the present invention, it is well known that performance is often measured in terms of FER for the forward and reverse links. At a fixed SNR, the FER may often be different at different mobile speeds. In order to obtain a FER indication the SNR should be mapped to the average FER under some wide range of mobility. At each value of SNR, define the weighted sum

$$\overline{FER} = \sum_i f_i w_i$$

where $\sum w_i = 1$, f_i is the FER at speed, v_i , the coefficient, w_i represents the weight assigned to the speed and \overline{FER} denotes the weighted average FER. By this technique it is possible to use the average metric to determine the SNR which in turn may be mapped to \overline{FER} .

[0036] As an example of an implemented rate adaptation system using the SNR measurements as a channel quality indicator. Let C_1, C_2, \dots, C_Q represent, in ascending order of bandwidth efficiency, the Q different modes of operation schemes for the transmitter. These different schemes may be implemented by using a fixed symbol rate and changing the trellis encoder and symbol mapper to pack a variable number of information bits per symbol. The upper bound on achievable throughput for each C_i at some SNR is given by $R(C_i)(1 - \overline{FER}(C_i, SNR))$ where $R(C_i)$ is the data rate corresponding to C_i in bits/second. The actual throughput can be lower as it also depends on higher recovery layers which

may time-out during retransmission.

[0037] FIG. 8, illustrates a graph having a three curves, with the vertical scale representing the \overline{FER} and the horizontal scale representing the SNR. The curves 154, 156, and 158 represent three hypothetical coded modulation schemes. For each coded modulation scheme, C_j , \overline{FER}_j is the average FER averaged over mobile speeds. As an example, associated with curve 156 is adaptation point A_j 160. If the SNR falls below this point the transmitter must change its mode from scheme C_j to scheme C_{j-1} and begin operation on curve 154, at B_{j-1} 155, corresponding to scheme C_{j-1} , above which C_j has lower throughput than C_{j-1} . The filtered Viterbi decoder metric may be used as an indicator of SNR at the mode adaptation point. For the j^{th} decoded block, set $M_j = \underline{M}_j$ or $M_j = \overline{M}_{j-1}$ depending on the choice of filter parameter.

[0038] θ_{high} and θ_{low} are the thresholds which depend on the filter parameter, α . Then, the adaptation rule for the data transmission is as follows: After the j^{th} block, if the transmitter is currently operating with C_j change the mode of operation to

$$C_{j-1}, \text{ if } \underline{M}_j / \mu_j > \theta_{high}, \text{ for } j = 2, 3, \dots, Q$$

and

$$C_{j+1}, \text{ if } \underline{M}_j / \mu_{j+r} < \theta_{low}, \text{ for } j = 1, 2, \dots, Q - 1$$

where $r = 1, 2, \dots, Q - j$. For each j , the highest allowable value of r maximizes the throughput by permitting a operation at a higher rate in bits per symbol. Finally, filtering of the metric can be applied across the coded modulation schemes since the metric average, μ , is independent of the mobile speed or the coded modulation scheme. Thus, there is no need to reset the channel quality measure after the adaptation.

[0039] Applying actual data to this example, FIG. 9 shows a table of values for a conservative mode adaptation strategy based on a Viterbi algorithm metric average. In, FIG. 9, C_1 , C_2 , and C_3 represent three coded modulation schemes where the choice of C_1 results in the lowest data rate and C_3 results in the highest data rate. Here, μ_1 , μ_2 and μ_3 are the target metrics corresponding to the \overline{FER} adaptation points for the three respective coded modulations. The thresholds θ_{high} and θ_{low} are defined such that θ_{high} is greater than 1.0 and θ_{low} less than 1.0. Additionally, FIG. 10 show a table of values for a aggressive mode adaptation strategy based on a Viterbi algorithm metric average.

[0040] A block diagram of an adaptive rate system for the invention is shown in FIG. 11. The diagram shows the possible implementation of the system at either the base station or the mobile station. The system operates in the following way. Initially, the system organizes the information to be transmitted into a transmit data stream 162. The transmit data stream 162 is then input into the transmitter 164 of the system. Within the transmitter 164, the transmit data stream 162 is encoded and modulated by the adaptive channel encoder and modulator 166. The encoding and modulation employed by the adaptive channel encoder and modulator 166 is controlled by the encoder and modulation decision unit 168. The encoder and modulation decision unit 168 determines the correct encoding and modulation scheme in response to the received SNR estimate 184 from the receiver 172. Initially, the encoder and modulation decision unit 168 chooses a predetermined scheme which is input to the adaptive channel encoder and modulator 166. The adaptive channel encoder and modulator 166 then encodes and modulates the transmit data stream 162 to a predetermined scheme and transmits the information through a channel 170 (possibly noisy and fading) to the receiver 172. After the information is received at the receiver 172 it is input into a channel decoder and demodulator 174 which produces two outputs. The first output of the channel decoder and demodulator 174 is a value of the Viterbi decoder metric 176 for the received information signal. The second output of the channel decoder and demodulator 174 is the received data stream 186 which will be the same as the information sent by the transmit data stream 162 a large fraction of the time. Next, the value of the Viterbi decoder metric 176 is averaged by an aggregate/averaging circuit 178 producing a moving average value for the Viterbi decoder metric 180. The moving average value for the Viterbi decoder metric 180 is then mapped to SNR estimate 184 by a mapping circuit 182. The resulting SNR estimate 184 is fed back into the encoder and modulation decision unit 168 to determine the encoder and modulation scheme to be used corresponding to the SNR estimate 184. The new scheme value of the encoder and modulation decision unit 168 is input into the adaptive channel encoder and modulator 166 which switches to the new encoding and modulation scheme for the transmit data stream 162 and transmits the information over the channel 170.

[0041] A block diagram of a system using the SNR to do power control is shown in FIG. 12. The diagram shows the possible implementation of the system at either the base station or the mobile station. The system operates in the following way. Initially, the system organizes the information to be transmitted into a transmit data stream 188. The transmit data stream 188 is then input into the transmitter 190 of the system. Within the transmitter 190, the transmit data stream 188 is encoded and modulated by the channel encoder and modulator 192. The transmit power level at

the channel encoder and modulator 192 is controlled by the power control algorithm circuit 212. The power control algorithm circuit 212 may determine the power control level in response to the received SNR estimate 210 from the receiver 196. Additionally, the power control algorithm circuit 212 may also determine the power control level in response to the signal strength and bit error rate estimate 200 from the receiver 196. Initially, the power control algorithm circuit 212 is set to a predetermined value which is input to the channel encoder and modulator 192. The channel encoder and modulator 192 then encodes and modulates the transmit data stream 188 using a predetermined encoding and modulation scheme and transmits the information at a predetermined power level through a channel 194 (possibly noisy and fading) to the receiver 196. After the information is received at the receiver 196 it is input into a channel decoder and demodulator 198 which produces three outputs. The first output of the channel decoder and demodulator 198 is a value of the Viterbi decoder metric 202 for the received information signal. The second output is estimates of the signal strength and bit error rate 200. The third output of the channel decoder and demodulator 198 is the received data stream 218 which should be the same as information sent by the transmit data stream 188. Next, the value of the Viterbi decoder metric 202 is averaged by an aggregate/averaging circuit 204 producing an average value for the Viterbi decoder metric 206. The average value for the Viterbi decoder metric 206 is then mapped to SNR estimate 210 by a mapping circuit 208. The resulting SNR estimate 210 is fed back into the power control algorithm circuit 212 to determine a power control value corresponding to the SNR estimate 210. The new power control value of the power control algorithm circuit 212 is input into the channel encoder and modulator 192 for use in subsequent transmissions of the data stream 188 over the channel 194 to the receiver.

[0042] Additionally, the mobile assisted handoff decision circuit 214 also processes the SNR estimate 210 and the signal strength and bit error rate estimates 200. If the SNR value is below a predetermined threshold the mobile assisted handoff decision circuit 214 sends a message to the handoff processor 216 to handoff the mobile station to a new base station.

[0043] In conclusion, the following summary should easily enable one skilled in the art to practice the invention. The first part of the invention is an apparatus for adaptively changing the modulation schemes of a transmit data stream based on the measured SNR of a channel. The adaptive modulation schemes are implemented in a transmitter by an adaptive channel encoder and modulator. An encoder and modulation decision unit is connected to the transmitter adaptive channel encoder and modulator to determine the correct encoding and modulation scheme based on the information received at the receiver. Then a receiver channel decoder and demodulator is placed in radio connection with the transmitter adaptive channel decoder and demodulator through the channel. This transmitter adaptive channel decoder and demodulator produces a path metric value which is averaged by an averaging circuit to produce an averaged path metric value. This averaged path metric value is then mapped through a mapping device to a SNR estimate value. The SNR estimate value is then input into the transmitter encoder and modulation decision unit to determine if the coding and modulation scheme should be changed in response to the SNR estimate value. It should be noted that the receiver channel decoder and modulator may be implemented in various way, however, in this example implementation a Viterbi decoder was used.

[0044] The second part of the invention is an apparatus for implementing mobile assisted handoff based on the measured SNR of a channel. The mobile assisted hand off is implemented in a transmitter by a channel encoder and modulator. A receiver channel decoder and demodulator is in radio connection with the transmitter channel decoder and demodulator through a channel. The receiver channel decoder and demodulator produces a path metric value in response to the information received by the receiver which is averaged by an averaging circuit to produce an averaged path metric value. This averaged path metric value is then mapped through a mapping device to a SNR estimate value. A power control algorithm circuit is connected to the transmitter channel encoder and modulator which varies the power level of the transmitter in response to the SNR estimate value. Finally, the SNR estimate value is input into a mobile assisted handoff decision unit which determines if the mobile station should perform a handoff operation based on the SNR estimate value. As in the first part of the invention, it should again be noted that the receiver channel decoder and modulator may be implemented in various way, however, in this example implementation a Viterbi decoder was used. Additionally, this second part of the invention can be either implemented at the mobile station or the base station.

[0045] Please note that while the specification in this invention is described in relation to certain implementations or embodiments, many details are set forth for the purpose of illustration. Thus, the foregoing merely illustrates the principles of the invention. For example, this invention may have other specific forms without departing from its spirit or essential characteristics. The described arrangements are illustrative and not restrictive. To those skilled in the art, the invention is susceptible to additional implementations or embodiments and certain of the details described in this application can be varied considerably without departing from the basic principles of the invention. It will thus be appreciated that those skilled in the art will be able to devise various arrangements which, although not explicitly described or shown herein, embody the principles of the invention and are thus within its spirit and scope. The scope of the invention is indicated by the attached claims.

Claims

1. A method for determining the signal to noise ratio, comprising the steps of:

5 establishing a set of path metrics corresponding to a set of predetermined signal to noise ratios;
receiving a digital signal;
determining a path metric for said digital signal; and
10 mapping said path metric to said corresponding signal to noise ratio in said set of predetermined signal noise to ratios.

15 2. The method of claim 1, wherein said digital signal is a coded signal.

3. The method of claim 1 wherein said digital signal is a trellis coded signal.

4. The method of claim 1 wherein the step of determining a path metric for said digital signal, further comprises the steps of:

20 establishing a set of signal to noise ratio values corresponding to a set of predetermined short term average of metric values, said short term average of metric values defined as M/μ ;
determining a decoded path metric from said received digital signal using a decoder, said decoded path metric defined as m_i ;
25 averaging m_i ; and
storing in a second memory unit said average decoded path metric, said average decoded path metric defined as μ ; and
30 determining an estimated Euclidean distance metric.

5. The method of claim 5 wherein the step of determining the estimated Euclidean distance metric is performed using the following equation:

$$M_i = \alpha M_{i-1} + (1-\alpha) m_i$$

40 where said estimated Euclidean distance metric is defined as M_i and α is a predetermined filter coefficient which is greater than zero and less than 1.0.

6. The method of claim 5 including the steps of:

45 determining a standard deviation of M_i ;
determining average metric thresholds defined as θ_{low} and θ_{high} based on said standard deviation of M_i ;
determining a value for M/μ by dividing said value of M_i by said value of μ ;
50 mapping said value of M/μ to a minimum value of said corresponding signal to noise ratio if M/μ is less than θ_{low} ;
mapping said value of M/μ to a maximum value of said corresponding signal to noise ratio if M/μ is greater than θ_{high} ; and
55 mapping said value of M/μ to said corresponding signal to noise ratio.

7. The method of claim 4 wherein said decoder is a Viterbi decoder for the maximum likelihood path.

8. A system for determining the signal to noise ratio, comprising:

- 5 means for establishing a set of path metrics corresponding to a set of predetermined signal to noise ratios;
- means for receiving a digital signal;
- means for determining a path metric for said digital signal; and
- 10 means for mapping said path metric to said corresponding signal to noise ratio in said set of predetermined signal noise to ratios.

9. The system of claim 1, wherein said digital signal is a coded signal.

10. The system of claim 1 wherein said digital signal is a trellis coded signal.

11. The system of claim 8 wherein the step of determining a path metric for said digital signal, further comprises:

- 20 means for establishing a set of signal to noise ratio values corresponding to a set of predetermined short term average of metric values, said short term average of metric values defined as M_i/μ ;
- means for determining a decoded path metric from said received digital signal using a decoder, said decoded path metric defined as m_i ;
- 25 means for averaging m_i ; and
- means for storing in a second memory unit said average decoded path metric, said average decoded path metric defined as μ ; and
- 30 means for determining an estimated Euclidean distance metric.

12. The system of claim 5 wherein the means for determining the estimated Euclidean distance metric is performed using the following equation:

35

$$M_i = \alpha M_{i-1} + (1-\alpha) m_i$$

40 where said estimated Euclidean distance metric is defined as M_i and α is a predetermined filter coefficient which is greater than zero and less than 1.0.

13. The system of claim 12 including the steps of:

- 45 means for determining a standard deviation of M_i ;
- means for determining average metric thresholds defined as θ_{low} and θ_{high} based on said standard deviation of M_i ;
- means for determining a value for M_i/μ by dividing said value of M_i by said value of μ ;
- 50 means for mapping said value of M_i/μ to a minimum value of said corresponding signal to noise ratio in said lookup table if M_i/μ is less than θ_{low} ;
- means for mapping said value of M_i/μ to a maximum value of said corresponding signal to noise ratio in said lookup table if M_i/μ is greater than θ_{high} ; and
- 55 means for mapping said value of M_i/μ to said corresponding signal to noise ratio.

14. The system of claim 4 wherein said decoder is a Viterbi decoder for the maximum likelihood path.

5

10

15

20

25

30

35

40

45

50

55

FIG. 1

PRIOR ART

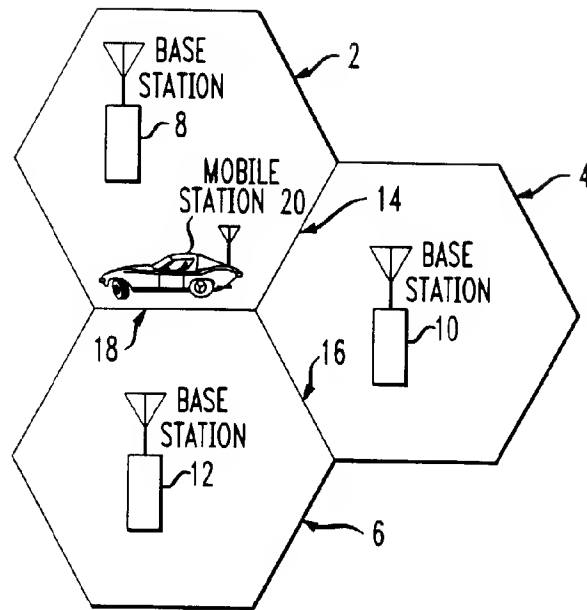


FIG. 2

PRIOR ART

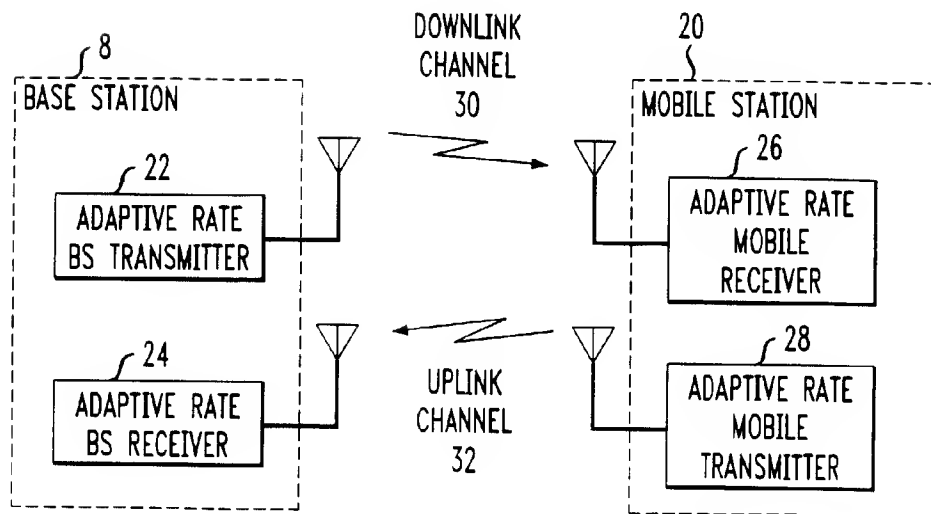


FIG. 3

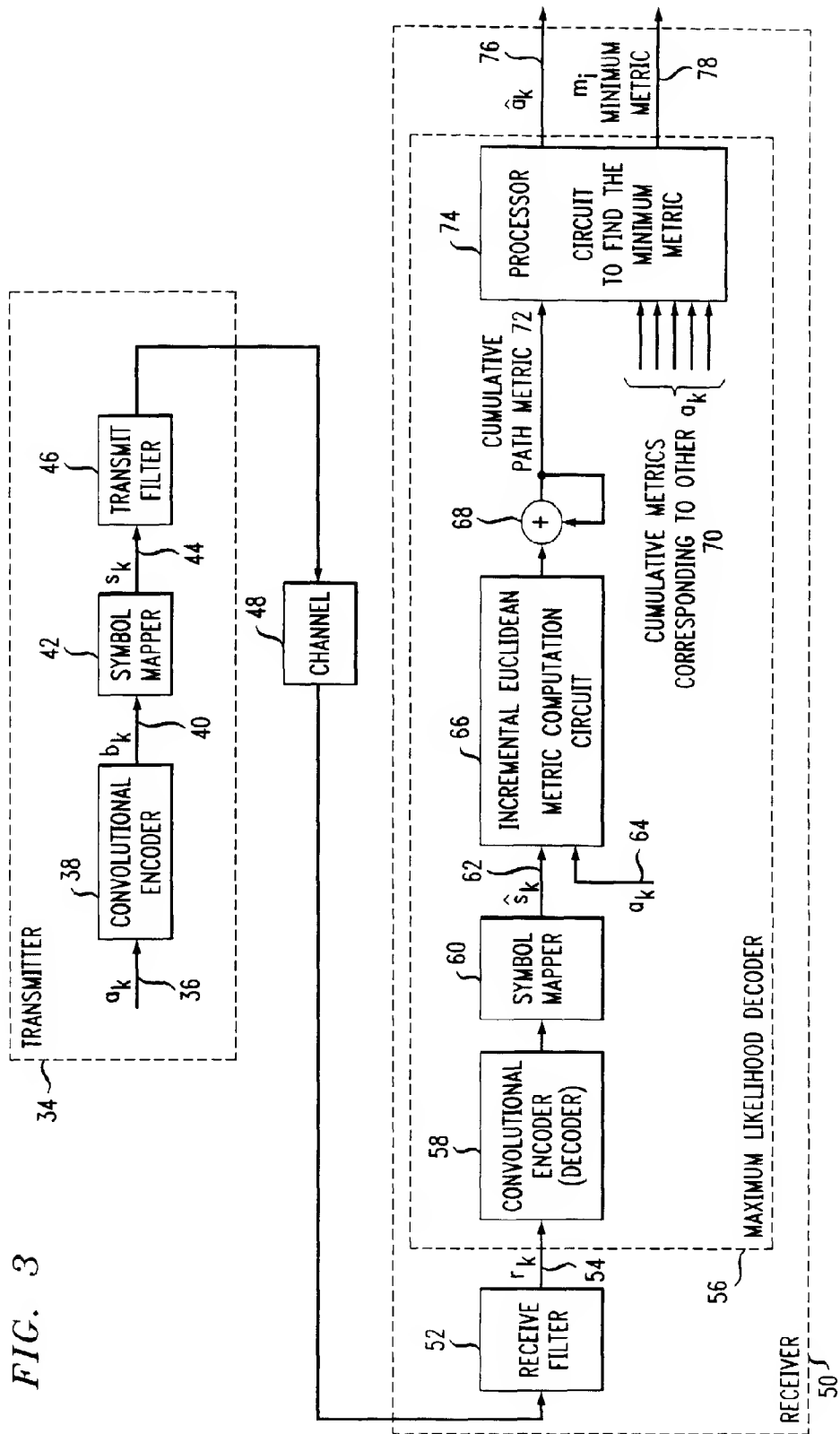


FIG. 4

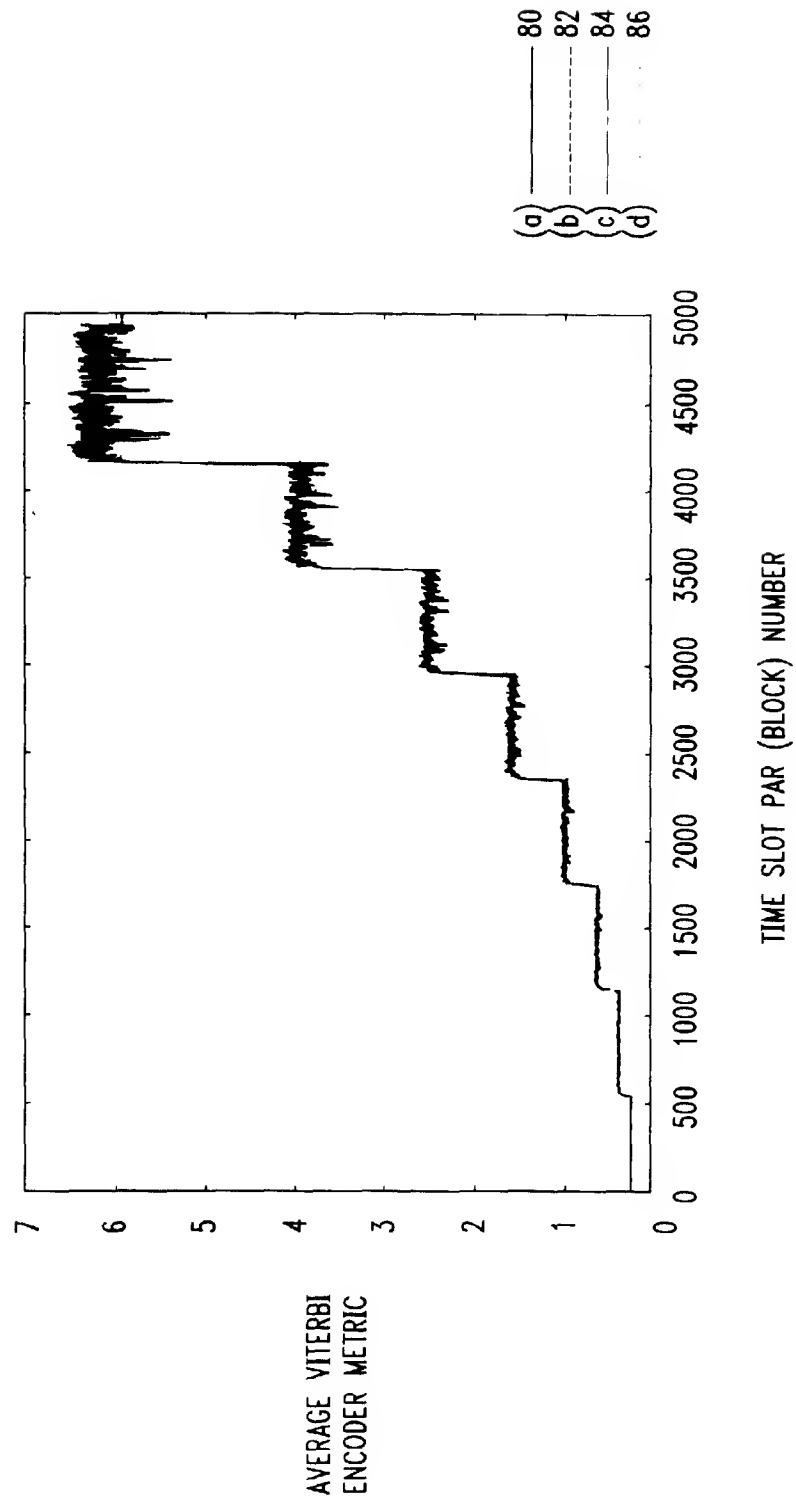


FIG. 5

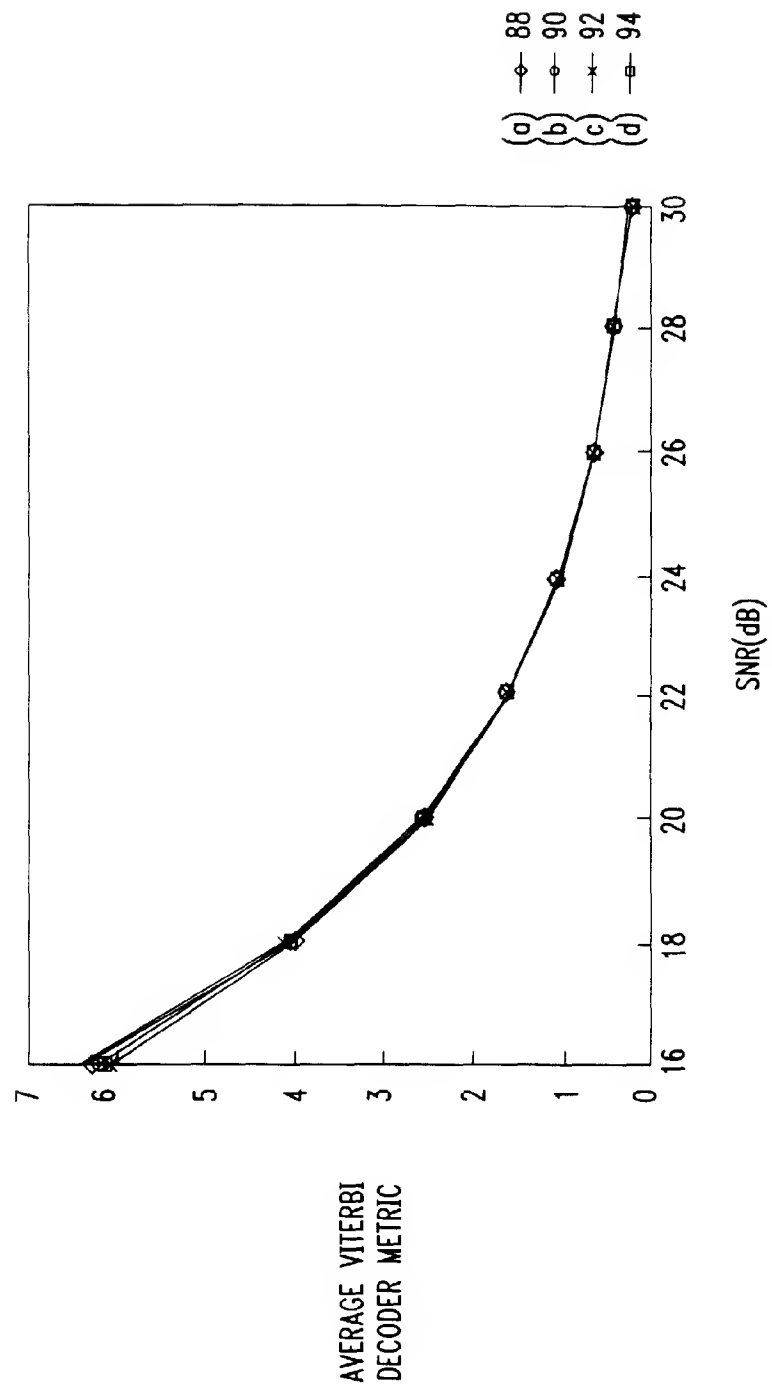


FIG. 6

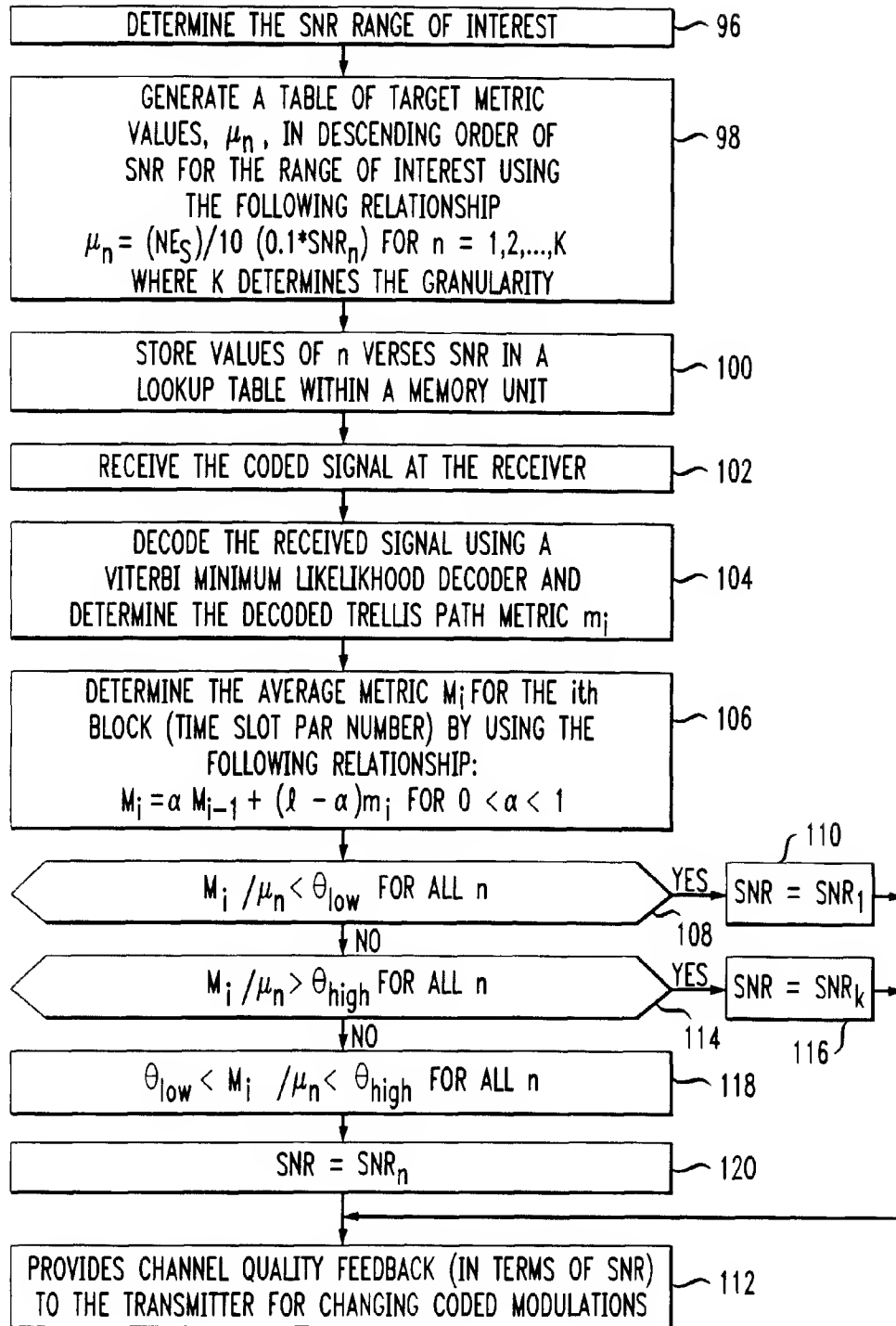


FIG. 7

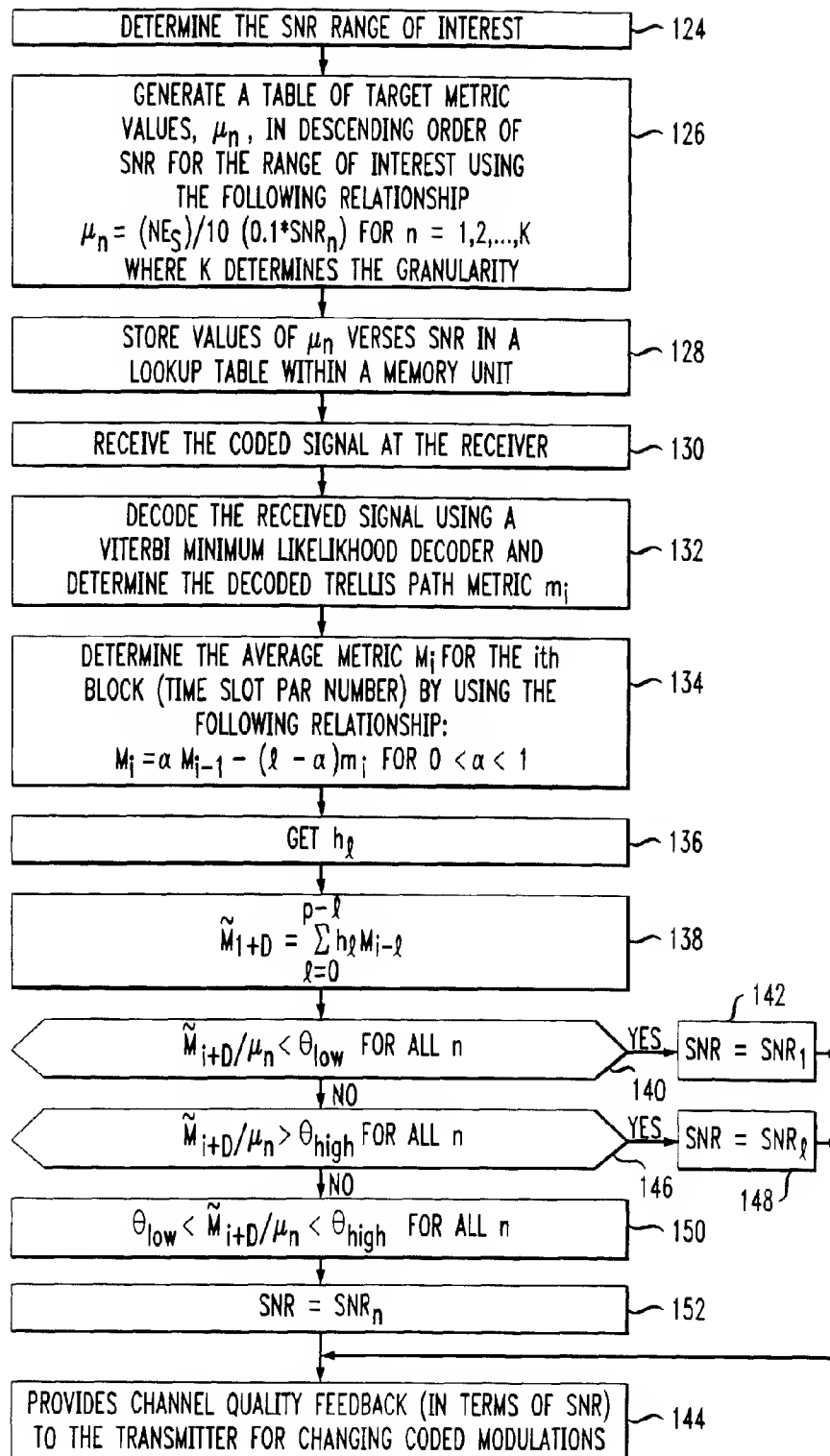


FIG. 8

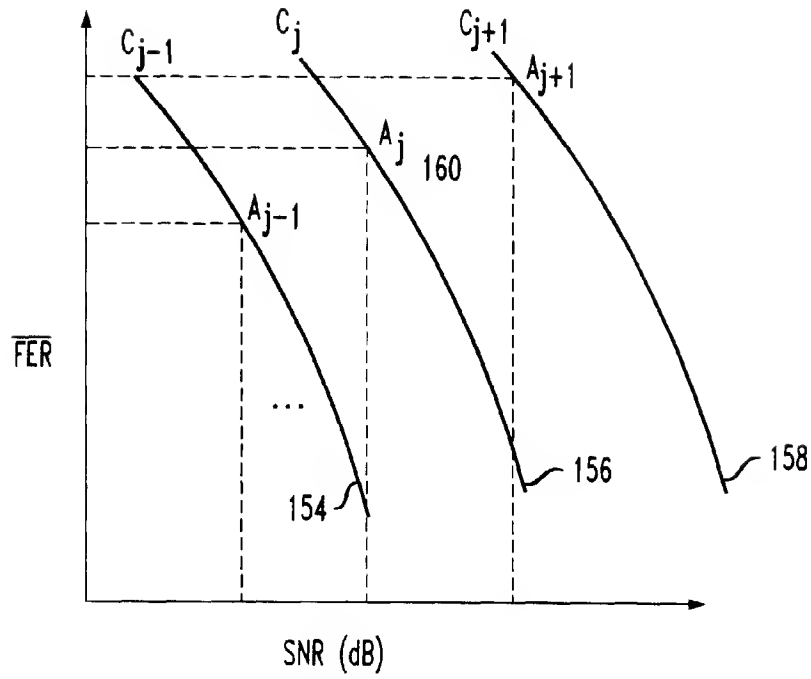


FIG. 9

CURRENT SCHEME	CONDITIONS ON METRIC	NEW SCHEME
C_1	$M_i/\mu_2 < \theta_{low}$	C_2
C_2	$M_i/\mu_3 > \theta_{high}$	C_1
	$M_i/\mu_3 < \theta_{low}$	C_3
C_3	$M_i/\mu_3 > \theta_{high}$	C_2

FIG. 10

CURRENT SCHEME	CONDITIONS ON METRIC	NEW SCHEME
C_1	$M_i/\mu_3 < \theta_{low}$	C_3
C_2	$M_i/\mu_2 > \theta_{high}$	C_1
	$M_i/\mu_3 < \theta_{low}$	C_3
C_3	$M_i/\mu_3 > \theta_{high}$	C_2

FIG. 11

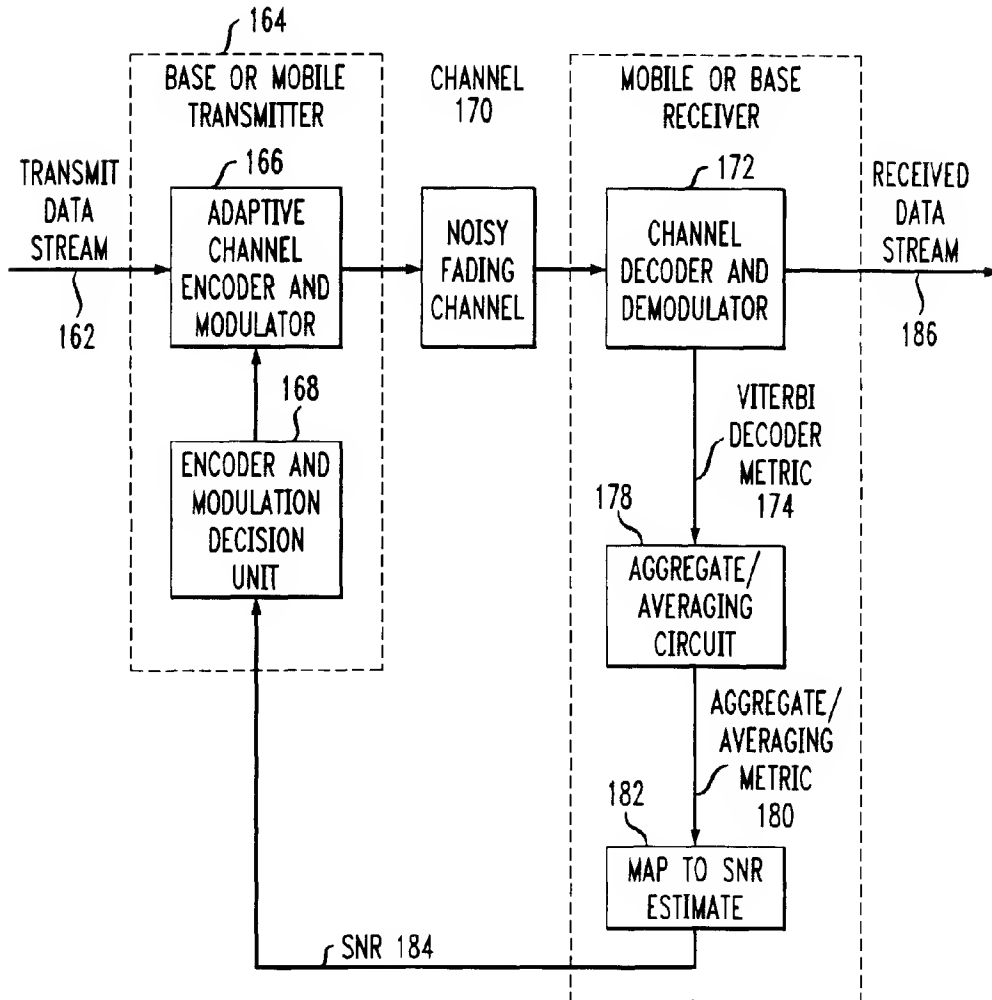


FIG. 12

